Vol 13 No 5, May 2004
1009-1963/2004/13(05)/0670-07

Chinese Physics

© 2004 Chin. Phys. Soc.
and IOP Publishing Ltd

Ionization for Hf- and W-L-shell by electron impact*

Yang Dai-Lun(杨代伦), Luo Xiao-Bing(罗小兵), Fu Yu-Chuan(傅玉川),
He Fu-Qing(何福庆), Long Xian-Guan(龙先灌),
Peng Xiu-Feng(彭秀峰)†, and Luo Zheng-Ming(罗正明)

Key Laboratory for Radiation Physics and Technology of the Education Ministry of China,
Institute of Nuclear Science and Technology, Sichuan University, Chengdu 610064, *China*

(Received 30 May 2003; revised manuscript received 26 November 2003)

Electron-induced Hf-, W-L-shell partial, total production cross sections, mean ionization cross sections and Hf-L_3-shell ionization cross sections (at two energies) have been measured as functions of electron energies (from near threshold to 36keV). The influence of electrons reflected from the backing of the thin targets on measured results was corrected using a model to relate to the electron transport process. The mean paths of electron multi-scattered in the target itself (including forward and backward scattering) were calculated by means of Monte Carlo program (EGS4) and they were used to correct measured results. A comparison with both theoretical predictions was given.

Keywords: tungsten, hafnium, L-shell ionization, electron impact
PACC: 3480D

1. Introduction

Inner shell ionization by electron impact has been attracting the attention of theoretical and experimental scientists. In the past many works focused essentially on K-shell ionization studies,[1−8] and works on L-shell ionization are still scarce. One of the reasons is the difficulty of preparation of thin element targets with a moderate thickness. By using the technique of thin element targets with a thick substrate, this difficulty can be surmounted; and using the above method, our group have recently carried out a few works: for example, the measurements on Hf-L-ionization [9] and Nb-L-ionization.[10]

However, electrons reflected from the substrate, when passing through the target film again, may reionize the target atoms, resulting in a systematic overestimation of the measured cross sections. Therefore, the influence of reflected electrons cannot be ignored. The influence of the substrate on measurements has been corrected using a bipartition model to deal with the electron transport process.[11]

In addition, incident lower-energy electrons may undergo multi-scattering when crossing the target layer. The multi-scattering would extend the mean electron path in the target, thus increase the x-ray counts and, as well as forward scattering electrons, some backward scattered electrons may exist near the threshold. Along the scattering paths the backward multi-scattered electrons may also ionize the target atoms to increase the observed x-ray counts. This effect could become serious if the incident electron energy is low (near the threshold) and the atomic number of the target element is high (for example, Hf, W). Therefore, the influence of both parts of the scattered electrons on the measured results must be considered. We have used the Electron Gamma Shower version 4 (EGS4) of the Monte Carlo method to calculate the contributions from multi-scatterings within the target. In our former report [12] on W-L-shell ionization the multi-scattering effects were not taken into consideration, hence the new data with the multi-scattering correction will also be given in the present paper.

2. Experimental details

The experimental setup used in the present study, in which an electron beam with energies between near threshold to 36keV is given by an electron gun, is the same as in Ref.[10]. A 60kV dc power supply was used to accelerate electrons from the electron gun. The

*Project supported in part by the National Natural Science Foundation of China (Grant No 19874045), and by the International Atomic Energy Agency, IAEA Research Contract No. 12354/RO/RBF.
†To whom correspondence should be addressed. E-mail: instpeng@scu.edu.cn

beam spot on the target was about 3mm in diameter. The horizontal dipstick of a Si(Li) detector was put inside the target chamber about 10cm from the centre of the target which was placed at 45° to the beam direction. The detector has an energy resolution of 180eV (full width at half maximum) at 5.9keV. Calibration of the efficiency of the detector system was carefully performed using a set of standard sources with 3% uncertainty, i.e. ^{241}Am, ^{137}Cs, ^{54}Mn. Targets were made by means of a heavy particle sputtering technique and furnished by the China Institute of Atomic Energy (Beijing). Target thickness was determined by direct weighing of a known area target, using a balance of high precision of 10^{-6}g in the institute. During experiment the gas pressure was kept at less than 3×10^{-3}Pa.

3. Data process

The L_α x-ray production cross section σ_α can be deduced by counting the numbers of L_α x-ray photons using the following formula:

$$\sigma_\alpha = \frac{4\pi A N_\alpha}{N_A N_e \rho\varepsilon\Omega(d/\cos\theta)}, \quad (1)$$

where A is the atomic number of the target, N_α the number of L_α x-ray photons, N_A the Avogadro constant, N_e the number of electrons hitting on the target; ρ (in g/cm^3) and d (in cm) are the density and geometrical thickness of the target, respectively; ε is the efficiency of the detector, Ω is the solid angle subtended by the beam spot to the detector effective area, θ is the angle between the incident electron beam and the normal of the target surface. The expressions of σ_β and σ_γ are similar to that of σ_α. The L-shell mean ionization cross section $\overline{\sigma}_L$ can be written as

$$\overline{\sigma}_L = \sigma_L/\overline{\omega}_L, \quad (2)$$

where σ_L is the total production cross section (by taking the sum of the three parts: σ_α, σ_β and σ_γ) and $\overline{\omega}_L$ is the L-shell mean fluorescence yield whose definition is as follows:[13]

$$\overline{\omega}_L = \frac{\omega_1^{ef}/I_1 + \omega_2^{ef}/I_2 + 2\omega_3^{ef}/I_3}{1/I_1 + 1/I_2 + 2/I_3}, \quad (3)$$

where I_i denotes the ionization energy of the ith subshell, the Coster–Kronig-corrected subshell effective fluorescence yields are evaluated using the following relations:

$$\omega_1^{ef} = \omega_1 + f_{12}\omega_2 + (f_{13} + f_{12}f_{23})\omega_3, \quad (4a)$$

$$\omega_2^{ef} = \omega_2 + f_{23}\omega_3, \quad (4b)$$

$$\omega_3^{ef} = \omega_3, \quad (4c)$$

with ω_i being the fluorescence yield for the ith subshell and f_{ij} the Coster–Kronig transition probability between the ith and jth subshells.

As mentioned above, the measured cross sections must be corrected for the electrons reflected from the substrate; the detail is published elsewhere.[1] The formula adopted for the correction is

$$\sigma_i(E) = \frac{4\pi A N_i}{N_A N_e \rho\varepsilon\Omega P} - \int_0^E \Phi_{ref}(E')\sigma_i(E')dE', \quad (5)$$

where $\sigma_i(E)$ and N_i are the production cross section and the count of the ith-group x-ray, and the suffix i represents α, β, and γ; P denotes the mean path length of the electrons suffered from multi-scattering (including the forward-, backward-scattering); and $\Phi_{ref}(E')$, the energy spectrum of the reflected electron at the surface of the substrate, can be evaluated by using the bipartition model of electron transport (see Ref.[1]).

4. Results and discussion

In the present experiment, the total uncertainty of production cross section is less than 14%, which consists mainly of the target thickness and its inhomogeneity (<5%), the detector efficiency (<4%), the beam integration (<3%), the counts (2–12%), and the uncertainties of constants used in the deduction of cross section have not been taken into account.

The partial production cross sections of L_α-, L_β-, L_γ-x-rays and the total production cross sections and the mean ionization cross sections of L-shell as functions of incident electron energy are shown in Figs.1 and 2. In Fig.2 only cross section energy relations of Hf, not of W, are given because both relations are similar. Some parameters used in calculating cross sections are presented in Tables 1 and 2. The results corrected for the substrate reflection and the multi-scattering within the target(including forward- and backward-scattering) are also given in Figs.1 and 2. Table 3 is a data list of multi-scattering correction, in which the data higher than 18 keV are not given, because the ratio, $P/(d/\cos\theta)$, has tended to unity for energies >18keV. The experimental cross sections of L_l x-rays have not been evaluated due to poor peak counts.

In addition, L_3-shell ionization cross sections σ_{L_3} can be deduced from L_α x-ray production cross sections σ_α. The cross section σ_α is a function of L_1-,

L_2-, and L_3-subshell ionization cross sections σ_{L_1}, σ_{L_2} and σ_{L_3} as follows:

$$\sigma_\alpha = \frac{\Gamma_{M4,5-L_3}}{\Gamma_{\text{total}-L_3}}\omega_3 \times [\sigma_{L_3} + f_{23}\sigma_{L_2} + (f_{13} + f_{12}f_{23})\sigma_{L_1}], \quad (6)$$

where $\Gamma_{M4,5-L_3}$and $\Gamma_{\text{total}-L_3}$ are the x-ray emission rates for L_α ($M_{4,5} - L_3$ transition) and total x-rays (M-, N-, O-L_3 transition) respectively; ω_3 is the fluorescence yield for the L_3-shell. For impact energies between L_3- and L_2-shell ionization energy (9.561, 10.739keV for Hf, respectively), σ_{L_1}, σ_{L_2} become zero and σ_{L_3} can be directly deduced from the production cross section σ_α. All the experimental data for Hf and W are given in Tables 4 and 5. The deduced Hf-L_3-shell ionization cross sections (at two energies) are given in Table 4b.

Table 1. Some parameters in deduction of the cross sections of Hf and W targets.

	Number of atom	Weight of atom	Density of target /(g/cm^3)	Mass-thickness of target /(μg/cm^2)	Mass-thickness of Al substrate /(mg/cm^2)
	Z	A	ρ	ρd	ρd
Hf	72	178.49	13.3	29.4	1.84
W	74	183.85	19.25	28.8	0.06

Table 2. Fluorescence (ω_i)[a], Coster–Kronig transition probability (f_{ij})[a], Ionization energy (I_i)[b] (in keV) and x-ray emission rate (Γ)[c] for Hf and W.

	ω_1	ω_2	ω_3	f_{12}	f_{13}	f_{23}	I_1	I_2	I_3
Hf	0.128	0.246	0.231	0.18	0.28	0.135	11.272	10.739	9.561
W	0.147	0.270	0.255	0.170	0.280	0.133	12.099	11.542	10.205
	$\Gamma_{\text{total-L1}}$	$\Gamma_{\text{total-L2}}$	$\Gamma_{\text{total-L3}}$	$\Gamma_{\text{M4-L3}}$	$\Gamma_{\text{M5-L3}}$	$\Gamma_{\text{M4-L2}}$	$\Gamma_{\text{M3-L1}}$	$\Gamma_{\text{M2-L1}}$	$\Gamma_{\text{N1-L3}}$
Hf	0.701	1.124	1.087	0.0896	0.791	0.995	0.2941	0.2281	0.0095
W	0.805	1.397	1.244	0.1018	0.898	1.138	0.330	0.2636	0.01119
	$\Gamma_{\text{N1-L2}}$	$\Gamma_{\text{N2-L1}}$	$\Gamma_{\text{N3-L1}}$	$\Gamma_{\text{N4-L2}}$	$\Gamma_{\text{N5-L3}}$	$\Gamma_{\text{O3-L3}}$	$\Gamma_{\text{O4-L2}}$	$\Gamma_{\text{O4,5-L3}}$	$\Gamma_{\text{O2-L1}}$
Hf	0.00653	0.0554	0.0752	0.1810	0.1374	0.01073	0.001934	0.001545	0.00792
W	0.00755	0.0647	0.0858	0.2118	0.1593	0.01288	0.00586	0.00468	0.01002

[a] taken from Ref.[14]; [b] taken from Ref.[15]; [c] taken from Ref.[16].

Table 3. The multi-scattering mean path length P calculated by using the Monte Carlo program for Hf and W*, and ratio R of mean path length P to the geometric thickness ($d/\cos\theta$) (in the present experiment θ=45° with respect to the incident electron beam)**

E/keV	T/%		(1-T)/%		t_1		t_2		R		$P/10^{-6}$cm	
	Hf	W	Hf	W	Hf	W	Hf	W	Hf	W	Hf	W
10.0	91.5		8.5		1.405		3.437		1.479		4.624	
10.5	92.5		7.5		1.375		3.471		1.440		4.503	
11.0	93.6	93.8	6.4	6.2	1.343	1.340	3.515	3.543	1.398	1.394	4.371	2.950
12.0	95.2	95.9	4.8	4.1	1.282	1.257	3.545	3.538	1.322	1.291	4.134	2.732
13.0	96.2	96.4	3.8	3.6	1.239	1.238	3.543	3.587	1.270	1.268	3.971	2.683
14.0	96.9	96.9	3.1	3.1	1.206	1.200	3.638	3.735	1.231	1.226	3.849	2.594
15.0		97.4		2.6		1.169		3.788		1.190		2.518
16.0	97.6	99.99	2.4	0.01	1.142	1.101	3.859	6.911	1.162	1.101	3.633	2.330
17.0		99.99		0.01		1.003		5.661		1.003		2.122
18.0	99.99		0.01		1.004		5.523		1.005		3.142	

*The normal geometric thicknesses d of the target are 2.211, 1.496 (in 10^{-6}cm) and (d/cos45°)=3.127, 2.116 (in 10^{-6}cm) for Hf and W respectively; $P/(d/\cos\theta)=R$.

**Symbols T and (1-T) are the transmittivity and the reflectivity of the incoming electron passing through the target respectively; t_1 and t_2 are the ratios of the geometric thickness $d/\cos\theta$, respectively, to forward-multi-scattering mean path P_f and backward-multi-scattering mean path P_b (i.e. $t_1 = P_f/(d/\cos\theta)$, $t_2 = P_b/(d/\cos\theta)$); $R = t_1t_2/[T(t_2 - t_1) + t_1]$ may be called the equivalent mean path ratio.

The binary encounter approximation (BEA) proposed by Gryzinski,[17] which is suitable for theoretical calculation of L-shell ionization cross section at present, can be written as

$$\sigma_i = b_i(\sigma_0/I_i^2)g_i(x), \tag{7}$$

with

$$g_i(x) = \frac{1}{x}\left(\frac{x-1}{x+1}\right)^{3/2} \times \left[1 + \frac{2}{3}\left(1 - \frac{1}{2x}\right)\ln\left[2.7 + (x-1)^{1/2}\right]\right],$$

where b_i is the number of electrons in the subshell L_i (i=1, 2 and 3), $x = E/I_i$, E is the incident electron energy, I_i is the ionization energy of the ith subshell, and σ_0=6.56×10^{-14}cm^2. This classical scaling apparently predicts the same value of $f(E/I_i)$ at the same E/I_i for all subshells.

Another theoretical calculation was proposed by McGuire [18] which can be written as

$$\sigma_i(I_i)^\alpha = f(E/I_i), \tag{8}$$

where $\alpha \neq 2$. This differs from the K-shell ionization, in which a simple scaling law $\sigma_{1s}(I_{1s})^2 = f(E/I_{1s})$ is adapted for all elements in the nonrelativistic limit. This nonclassical scaling law predicts the same feature of $f(E/I_i)$ only when the subshells have the same orbital angular momentum, such as $2p_{1/2}$ and $2p_{3/2}$.

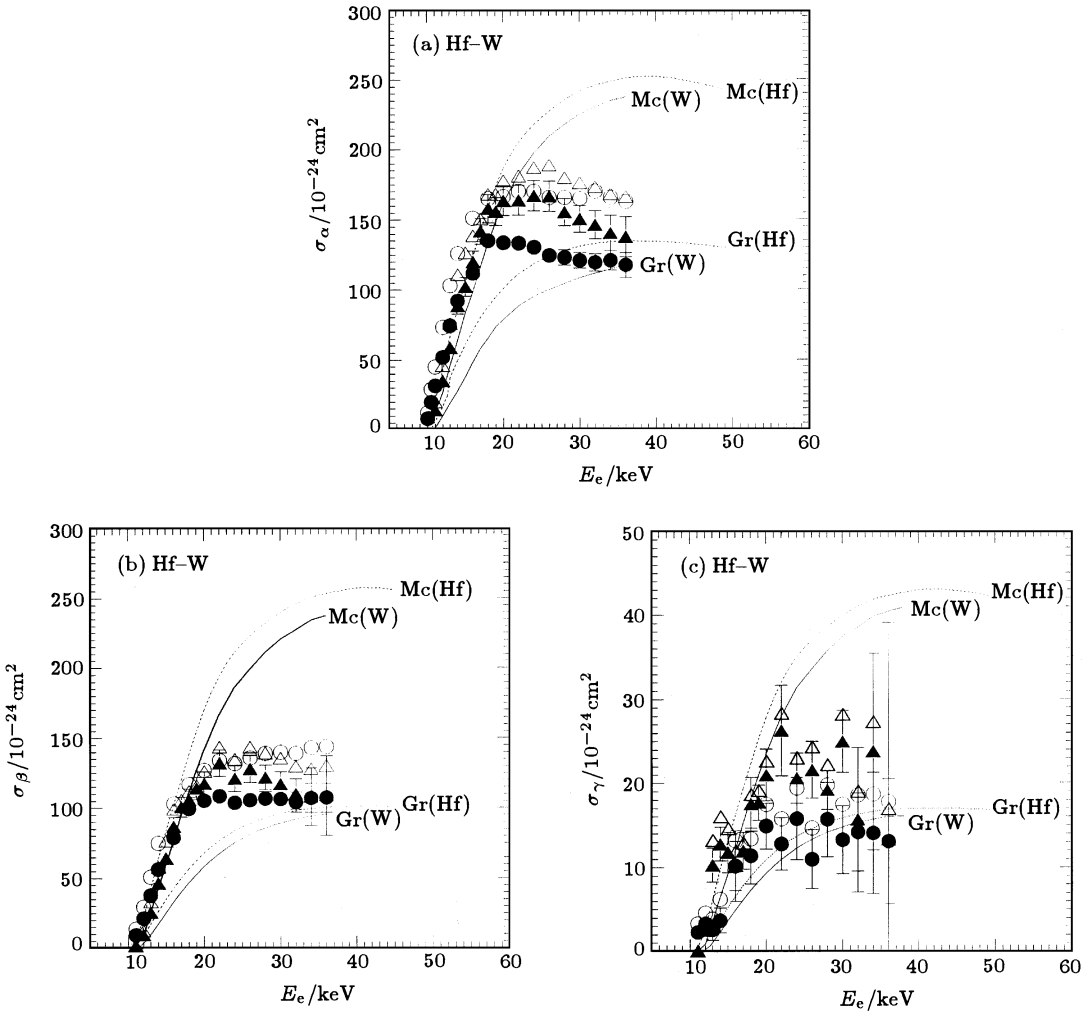


Fig.1. L-shell cross sections versus electron energy: experimental values of (a) L_α-ray, (b) L_β-ray, and (c) L_γ-ray production cross sections. The letters Mc and Gr represent, respectively, McGuire's and Gryzinski's theories. Open and solid triangles, respectively, represent the original values and the values corrected on both substrate and multi-scattering effects for W. Open and solid circles are the original values and the values corrected on both substrate and multi-scattering effects for Hf.

For comparison with experimental values we have made calculations using the above two predications, from which we only obtained the ionization cross sections of the three subshells L_1, L_2, L_3 of hafnium and tungsten, therefore we have to convert them into production cross sections to benefit from comparison with the measured production cross sections. The above-mentioned conversion formulae can be acquired from Ref.[11] and the emission rates adopted in the conversion calculation are also given in Table 2. The calculated graphs for both predictions are also shown in Figs.1 and 2.

From Figs.1 and 2 we can conclude that the near-threshold experimental values are very close to the predictions by McGuire provided that both corrections of the substrate reflection and multi-scattering have been made, and at higher energies the corrected experimental results tend to the predictions by Gryzinski, but the corrected measured values are still higher than the theoretical predictions at near threshold. Therefore, more work on lower-energy electron impact may be necessary. In addition, we can greatly extend the investigating range by means of the method of thin target with thick substrate, but the effect of reflection of electrons from the substrate must be corrected. When the target of a higher atomic number is bombarded by lower-energy electrons, the influence of multi-scattering within the target on experimental results is very serious and thus must be corrected. To our knowledge, this is the first time that account has been taken of the backward multi-scattering electron by using the Monte Carlo method. In this way a good agreement between experimental and theoretical calculation can be achieved.

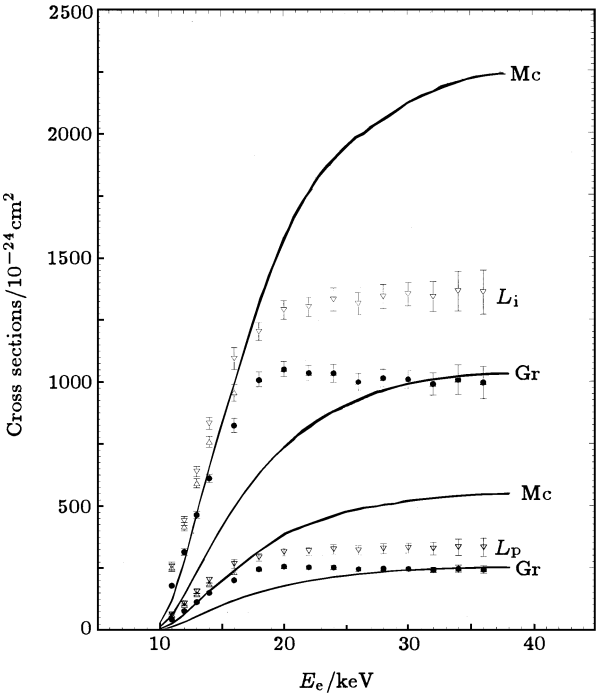


Fig.2. Total production cross sections (Lp) and mean ionization cross sections (L_i) of element Hf versus electron impact energy. Open triangles indicate the original values (down), the values corrected on substrate effect (up), and solid circles are experimental values corrected on the multi-scattering effect. Other symbols are as in Fig.1.

Table 4a. Measured values of partial production cross sections of electron-induced Hf-L-shell ionization* and their errors (in 10^{-24}cm^2).

	L_α			L_β			L_γ		
E/keV	σ_α	$\sigma_{\alpha 1}$	$\sigma_{\alpha 2}$	σ_β	$\sigma_{\beta 1}$	$\sigma_{\beta 2}$	σ_γ	$\sigma_{\gamma 1}$	$\sigma_{\gamma 2}$
10.0	12.7±1.4	12.6±1.3	8.4±1.0						
10.5	30.4±2.6	29.9±2.6	20.8±1.8						
11.0	46.7±2.8	45.3±2.7	32.4±1.9	13.7±2.2	13.2±2.1	9.4±1.5	3.3±1.1	3.2±1.0	2.3±0.8
12.0	74.2±3.3	69.9±3.0	52.8±2.3	29.3±2.9	28.2±2.8	21.4±2.1	4.6±0.9	4.3±0.8	3.3±0.7
13.0	101.8±3.6	93.8±3.3	73.5±2.6	51.1±3.1	48.2±2.9	37.9±2.3	3.9±2.0	3.3±1.7	2.6±1.3
14.0	123.0±3.9	110.8±3.5	90.0±2.9	75.2±3.6	69.8±3.3	56.7±2.7	6.2±2.5	5.5±2.2	3.7±1.5
16.0	152.0±5.6	130.9±4.8	112.7±4.2	103.3±5.0	91.9±4.4	79.2±3.8	13.2±7.8	11.9±5.0	10.2±4.2
18.0	164.7±6.1	136.8±5.1	136.1±5.1	117.1±5.2	100.1±4.4	99.6±4.4	13.4±3.8	11.5±3.3	11.4±3.3
20.0	171.8±5.9	137.7±4.7	137.5±4.7	127.1±6.2	105.4±5.1	105.4±5.1	17.5±3.2	14.9±2.7	14.9±2.7
22.0	169.7±6.3	132.8±4.9	132.8±4.9	134.0±5.8	108.4±4.7	108.4±4.7	15.8±3.8	12.8±3.1	12.8±3.1
24.0	175.3±7.0	134.4±5.4	134.4±5.4	132.4±6.4	104.0±5.0	104.0±5.0	19.4±6.0	15.8±4.9	15.8±4.9
26.0	171.8±7.1	128.1±5.4	128.1±5.4	135.8±6.6	105.3±5.1	105.3±5.1	14.7±4.7	11.0±3.5	11.0±3.5
28.0	170.4±7.6	126.4±5.7	126.4±5.7	139.0±6.9	106.6±5.3	106.6±5.3	19.8±5.6	15.7±4.4	15.7±4.4
30.0	173.9±8.1	127.6±6.0	127.6±6.0	140.2±6.3	106.4±4.8	106.4±4.8	17.5±5.3	13.3±4.0	13.3±4.0
32.0	171.1±9.1	124.6±6.6	124.6±6.6	138.7±9.8	103.9±7.3	103.9±7.3	18.6±6.0	14.2±4.6	14.2±4.6
34.0	172.5±9.8	125.6±7.1	125.6±7.1	143.3±13.7	107.2±10.2	107.2±10.2	18.7±9.5	14.1±7.2	14.1±7.2
36.0	171.4±13.0	124.8±9.5	124.8±9.5	144.1±13.9	107.5±10.4	107.5±10.4	17.8±10.1	13.1±7.4	13.1±7.4

Table 4b. The measured results and their errors of Hf target ionization by electron impact.

E/keV	σ_{L3} (10^{-24}cm^2)			σ_L (10^{-24}cm^2)			$\overline{\sigma}_L$ (10^{-24}cm^2)		
	uncorrected	corrected for backing	corrected for multiple-scattering	uncorrected	corrected for backing	corrected for multiple-scattering	uncorrected	corrected for backing	corrected for multiple-scattering
10.0	67.9±7.5	67.4±7.4	45.6±5.0						
10.5	162.4±13.9	159.6±13.7	110.8±9.5						
11.0				63.7±6.1	61.7±5.9	44.1±4.2	260.0±24.9	251.6±24.1	179.8±17.1
12.0				108.1±7.1	102.4±6.7	77.5±5.1	441.2±29.0	418.1±27.3	316.6±20.8
13.0				156.8±8.7	145.3±8.1	114.4±6.4	640.0±35.5	593.1±33.1	464.9±26.1
14.0				204.4±10.0	186.1±9.1	150.4±7.4	834.3±40.8	759.6±37.1	613.9±30.2
16.0				268.5±18.4	234.7±16.1	202.0±13.9	1096±75.1	958.0±65.7	824.5±56.7
18.0				295.2±15.1	248.4±12.7	246.9±12.6	1205±61.6	1014±51.8	1008±51.4
20.0				316.4±15.3	258.0±12.5	257.8±12.5	1290±62.4	1053±51.0	1052±51.0
22.0				319.5±15.9	254.0±12.6	254.0±12.6	1304±64.9	1037±51.4	1037±51.4
24.0				327.1±19.4	254.1±15.1	254.1±15.1	1335±79.2	1037±61.6	1037±61.6
26.0				322.3±18.4	245.7±14.0	245.7±14.0	1316±75.1	1003±57.1	1003±57.1
28.0				329.2±20.1	248.7±15.2	248.7±15.2	1344±82.0	1015±62.0	1015±62.0
30.0				331.6±19.7	247.3±14.7	247.3±14.7	1353±80.4	1009±60.0	1009±60.0
32.0				328.4±24.9	242.7±18.4	242.7±18.4	1340±102	990.6±75.1	990.6±75.1
34.0				334.5±33.0	247.1±24.4	247.1±24.4	1365±135	1009±99.6	1009±99.6
36.0				333.3±37.0	245.4±27.2	245.4±27.2	1360±151	1002±111	1002±111

Table 5a. Measured values of partial production cross sections of electron-induced W-L-shell ionization* and their errors (in 10^{-24}cm^2).

	L_α			L_β			L_γ		
E/keV	σ_α	$\sigma_{\alpha1}$	$\sigma_{\alpha2}$	σ_β	$\sigma_{\beta1}$	$\sigma_{\beta2}$	σ_γ	$\sigma_{\gamma1}$	$\sigma_{\gamma2}$
11.0	20.1±1.8	20.0±1.8	14.3±1.3	1.92±1.5	1.91±1.5	1.4±1.1			
12.0	46.1±3.4	45.5±1.8	35.2±2.6	12.3±2.5	12.2±2.5	9.4±1.9	2.2±0.5	2.2±0.5	1.7±0.4
13.0	75.9±5.0	74.4±4.9	58.7±3.9	33.1±3.1	32.6±3.0	25.7±2.4	6.1±1.2	6.1±1.2	4.8±0.9
14.0	111.0±7.2	108.1±7.0	88.2±5.7	58.0±4.5	56.8±4.4	46.3±3.6	11.4±1.8	11.2±1.8	9.1±1.4
15.0	126.4±8.2	121.7±7.9	101.7±6.7	76.8±5.7	74.6±5.5	64.3±4.7	12.8±2.6	12.4±2.6	10.4±2.1
16.0	138.6±9.0	132.1±8.6	120.1±7.8	99.2±7.0	95.7±6.8	86.9±6.2	3.3±3.6	12.5±3.5	11.4±3.2
17.0	150.7±9.6	142.3±9.1	141.9±9.1	105.8±7.3	101.0±6.9	100.7±6.9	14.1±2.6	13.1±2.4	13.1±2.4
18.0	168.3±10.6	157.9±9.8	157.9±9.8	111.9±7.7	105.8±7.3	105.8±7.3	15.7±2.9	14.8±2.7	14.8±2.7
19.0	168.0±10.6	155.8±9.8	155.8±9.8	121.6±8.0	114.1±7.5	114.1±7.5	17.4±2.1	16.1±1.9	16.1±1.9
20.0	177.5±11.5	163.5±10.6	163.5±10.6	126.3±8.7	117.4±8.1	117.4±8.1	20.2±3.0	18.8±2.8	18.8±2.8
22.0	181.1±11.6	163.9±10.6	163.5±10.6	143.7±9.6	132.2±8.9	132.2±8.9	22.5±4.6	20.9±4.3	20.9±4.3
24.0	187.1±12.0	167.1±10.7	167.1±10.7	135.0±9.3	121.3±8.4	121.3±8.4	23.0±3.4	21.0±3.0	21.0±3.0
26.0	189.1±12.1	166.7±10.7	166.7±10.7	143.7±9.6	128.1±8.6	128.1±8.6	24.3±3.8	21.6±3.4	21.6±3.4
28.0	179.7±11.1	155.4±9.6	155.4±9.6	139.5±8.7	122.3±7.6	122.3±7.6	22.2±2.6	19.2±2.3	19.2±2.3
30.0	176.1±11.1	150.4±9.5	150.4±9.5	135.7±9.1	117.2±7.9	117.2±7.9	19.8±2.9	17.5±2.6	17.5±2.6
32.0	173.2±12.0	146.3±10.0	146.3±10.0	129.7±11.0	110.3±9.2	110.3±9.2	19.0±10.4	15.7±8.6	15.7±8.6
34.0	168.1±14.9	140.3±12.5	140.3±12.5	128.1±20.5	107.9±17.3	107.9±17.3	17.5±8.2	15.2±7.5	15.2±7.5

Table 5b. Measured results of W-L-shell total production cross sections and mean ionization cross sections, and their errors.

E/keV	σ_L (10^{-24}cm^2)			$\overline{\sigma}_L$ (10^{-24}cm^2)		
	uncorrected	corrected for backing	corrected for multiple-scattering	uncorrected	corrected for backing	corrected for multiple-scattering
11.0	22.0±3.3	21.9±3.3	15.7±2.4	81.5±12.2	81.1±12.2	58.1±8.9
12..0	60.6±6.4	59.9±4.8	46.3±4.9	224.4±23.7	221.9±17.8	171.5±18.1
13..0	115.1±9.3	113.1±9.1	89.2±7.2	426.3±34.4	418.9±33.7	330.4±26.7
14..0	180.4±13.5	176.1±13.2	143.6±10.7	668.1±50.0	652.2±48.9	531.9±39.6
15..0	216.0±16.5	208.7±16.0	176.4±13.5	800.0±61.1	772.9±59.2	653.3±50.0
16..0	251.1±19.6	242.3±18.9	218.4±17.2	930.0±72.6	897.4±70.0	808.9±63.7
17..0	270.6±19.5	256.4±18.4	255.7±18.4	1002±72.2	949.6±68.1	947.0±68.1
18..0	296.0±21.2	276.8±19.6	276.8±19.6	1096±78.5	1025±72.6	1025±72.6
19..0	307.4±20.7	286.1±19.2	286.1±19.2	1138±76.7	1060±71.1	1060±71.1
20..0	324.2±23.2	299.8±21.5	299.8±21.5	1201±85.9	1110±79.6	1110±79.6
22..0	347.5±25.8	316.9±23.8	316.9±23.8	1287±95.6	1174±88.1	1174±88.1
24..0	345.0±24.7	309.0±22.1	309.0±22.1	1278±91.5	1144±81.9	1144±81.9
26..0	357.3±25.5	316.6±22.7	316.6±22.7	1323±94.4	1172±84.1	1172±84.1
28..0	340.2±22.4	296.2±19.5	296.2±19.5	1260±83.0	1097±72.2	1097±72.2
30..0	331.8±23.1	284.5±20.0	284.5±20.0	1229±85.6	1054±74.1	1054±74.1
32.0	322.0±33.4	271.7±27.8	271.8±27.8	1192±124	1006±103	1008±103
34.0	313.5±43.6	263.2±37.3	263.2±37.3	1161±161	974.8±138	974.8±138

In Tables 4 and 5 the symbol σ_i (i represents α, β, γ) indicates primary value, the symbols σ_{i1} and σ_{i2} mean, respectively, the values corrected for substrate and for multiple scattering.

References

[1] Luo Z M, An Z, He F Q, Li T H, Long X G and Peng X F 1996 *J. Phys.* B **29** 4001

[2] An Z, Luo Z M, Li T H and Wang L M 1996 *Phys. Rev.* A **54** 3067

[3] Peng X F, He F Q, Long X G, Luo Z M and An Z 1998 *Phys. Rev.* A **58** 2034

[4] Luo Z M, Tang C H, An Z, He F Q, Peng X F and Long X G 2001 *Phys. Rev.* A **A63** 4702

[5] He F Q, Long X G, Peng X F, Luo Z M and An Z 1996 *Chin. Phys. Lett.* **13** 175

[6] Tang C H, Luo Z M, An Z and Li T H 1999 *Chin. Phys. Lett.* **16** 505

[7] Zhou C G, Fu Y C, An Z, Tang C H and Luo Z M 2001 *Chin. Phys. Lett.* **18** 531

[8] Liu M T, An Z, Luo Z M, Peng X F and Long X G 2000 *At. Data and Nucl. Data Tables* **76** 213

[9] Luo Z M, Fu Y C, An Z, Peng X F, He F Q and Long X G 2002 *Chin. Phys. Lett.* **19** 1610

[10] Peng X F, He F Q, Long X G, An Z and Luo Z M 2001 *Chin. Phys.* **10** 31

[11] Luo Z M 1985 *Phys. Rev.* B **32** 812; B **32** 824

[12] Peng X F, He F Q, Long X G, An Z and Luo Z M 2000 *Chin. Phys.* **9** 749

[13] For example Ishii K *et al* 1977 *Phys. Rev.* A **15** 906

[14] Krause M O 1979 *J. Phys. Chem. Ref. Data* **8** 307

[15] Liu Y Z *et al* 1982 *The Decay Scheme for Usual Radionuclides* (Beijing: Atomic Energy Press) p400 (in Chinese)

[16] Scofield J H 1974 *At. Data and Nucl. Data Tables* **14** 121

[17] Gryzinski M 1965 *Phys. Rev.* A **138** 336

[18] McGuire E J 1977 *Phys. Rev.* A **16** 73